Morad Taher[1], Taoufik Mourabit[2], Issam Etebaai[3], Hinde Cherkaoui Dekkaki[4],
Najat Amarjouf[5], Afaf Amine[6], Bourjila Abdelhak[7], Ali Errahmouni[8], Sadik Azzouzi[9]

# Identification of Groundwater Potential Zones (GWPZ) Using Geospatial Techniques and AHP Method: a Case Study of the Boudinar Basin, Rif Belt (Morocco)

**Abstract:** The present study aims to delineate the groundwater potential zones (GWPZ) in the Boudinar Basin using geospatial techniques and through an analytical hierarchal process (AHP) method. For multi criteria decision analysis, fifteen thematic layers were integrated into a geographic information system (GIS) environment. In this analysis, each thematic layer is calculated for normalized weights. Furthermore, the consistency index and consistency ratio were calculated to ensure that the result was significant and reliable. The GWPZ map has been categorized into three classes: poor (50.82%), moderate (49.06%), and good (<1.00%). To compare the result, we used four other scenarios of the GWPZ. Two of them are the most similar to our result. Finally, predictive groundwater production and management strategies that ensure long-term sustainability are highly needed.

[1] Abdelmalek Essaadi University, FSTH, Applied Geosciences and Geological Engineering Research Team, Tétouan, Morocco, email: m.taher@uae.ac.ma (corresponding author), https://orcid.org/0000-0002-9273-2764
[2] Abdelmalek Essaadi University, Morocco, https://orcid.org/0000-0002-5542-7074
[3] Abdelmalek Essaadi University, Morocco, https://orcid.org/0000-0001-5941-656X
[4] Abdelmalek Essaadi University, Morocco, https://orcid.org/0000-0002-7501-0604
[5] Abdelmalek Essaadi University, Morocco, https://orcid.org/0000-0002-5147-3188
[6] Mohammed V University in Rabat, Morocco, https://orcid.org/0000-0002-9304-3987
[7] Abdelmalek Essaadi University, Morocco, https://orcid.org/0000-0003-2592-6179
[8] Abdelmalek Essaadi University, Morocco, https://orcid.org/0000-0003-0303-8971
[9] Mohammed first University, Morocco, https://orcid.org/0000-0002-3110-4262

## 1.   Introduction

Groundwater, a vital capital, is used by about 2.5 billion human beings for drinking, irrigation and many other activities [1]. Globally, the irrational use of groundwater has depleted it [2]. Furthermore, population growth and climate change can lead to groundwater scarcity [3]. Therefore, the sustainable management of groundwater is needed to avoid a global water crisis, especially in developing countries.

In Africa, where rapid population growth is occuring, water resources are among the lowest in the world and are expected to fall over 50% by 2050, according to the food and agriculture organization of the United Nations (FAO). Despite many studies having identified the potential groundwater in African countries: Ethiopia [4], Mali [5], Egypt [6], Morocco [7, 8], Nigeria [9], the mapping and estimation of groundwater recharge are still required to avoid water scarcity.

In Morocco, climate change has increased the risk of water scarcity [10]. Furthermore, the increased demand for water for drinking and agriculture purposes has also increased, especially in southern Morocco, where 65% of irrigation water for irrigation supplies comes from groundwater [11]. In northern Morocco, the tourism activities in coastal regions in summer increase the water consumption. In addition, the pollution from households, industry and agriculture has all aggravated the groundwater situation in Morocco [10, 12].

In the Rif Belt, soil erosion is a major factor leading to the siltation of dams and reducing their storage capacity [13]. Moreover, the scarcity of precipitation in recent decades has led to an overuse of groundwater resources for irrigation. Using remote sensing (RS) and geographic information systems (GIS), a number of researchers have identified and estimated groundwater potential zones (GWPZ) in the Rif: Ghis Basin [14], Nekor Basin [15], and the Bokoya Massif [16] to mitigate the lack of potable water in the Rif region. The Boudinar Basin was chosen for this study because the groundwater in this area constitutes the only source of water for both drinking and irrigation. Furthermore, the mentioned area remains unexplored in terms of hydrogeological research.

Traditional groundwater exploration techniques, such as drilling, geological, borehole data, geophysical methods, and field surveys, are costly, require extensive labor, and are time-consuming [17–19]. Alternatively, modern technologies such as geographic information systems, remote sensing, AHP, and multi-criteria decision-making analysis approaches (MCDA) have become essential techniques, as they are less expensive, more responsive, and more convenient. They have been widely used for GWPZ [17–20]. The Analytical Hierarchy Process (AHP) technique is an excellent approach for calculating output consistency, decreasing bias, and applying it in different environments [6]. It is beneficial to find each criterion and their respective features by pairwise comparisons [18]. Furthermore, the multicriteria decision analysis (MCDA) technique is employed in complex decision-making

problems, including GWPZ [18]. The groundwater prospection zones are based mainly on the integrations of multiple criteria such as stream networks, topography, lithology, slope steepness, and the frequency of lineaments [6].

The present study aims to delineate the GWPZ in the Boudinar Basin using geospatial techniques and the analytical hierarchy process (AHP) method as new approaches used in this study since, to the best of our knowledge, they have never been investigated in the study area, which means the absence of results comparison. This methodology was chosen because of the high percentage of conformity obtained during the validation of GWPZs studies, its efficiency and low cost in the delineation of GWPZs (Tab. 1) [21]. This objective was achieved by preparing and combining layers of 15 parameters that control groundwater recharge: altitude, slope, lithology, lineament density, drainage density, plan curvature, profile curvature, soil, topographic witness index (TWI), rainfall, distance from river, distance from fault, land use land cover (LULC), roughness and normalized difference vegetation index (NDVI). Given that the Boudinar Basin is an agriculturally oriented rural area, GWPZ mapping is crucial for its long-term economic growth.

**Table 1.** Percentages of conformity obtained during the validation of GWPZs studies

| Authors | Year | Country | Study area | Conformity [%] |
|---------|------|---------|-----------|----------------|
| [10] | 2022 | Morocco | Tata Basin | 80 |
| [22] | 2022 | Cameroun | Yoyo Basin | 79–87 |
| [23] | 2022 | South Africa | Kwazulu-Natal | 72 |
| [14] | 2021 | Morocco | Ghis Basin | 70 |
| [24] | 2021 | Turkey | Central Antalya | 56 |
| [25] | 2021 | Ethiopia | Abay Basin | 82 |
| [26] | 2021 | Sri Lanka | Kilinochchi | 81 |
| [27] | 2021 | India | Kashmir Valley | 79 |
| [28] | 2020 | Iraq | Ali Al-Gharbi | 76 |
| [29] | 2019 | India | Chittar Basin | 71 |

## 2.  Study Area

The Boudinar Basin is located in the north-eastern part of Morocco (Fig. 1), its territory belongs to the Driouch province, and it covers the following municipalities: Trougout, Boudinar, Beni Marghnin, Talilit, Temsaman, Ijarmaouas and Iferni. The GIS-based delimitation of the Boudinar Basin has a total area of 350 km². The basin

stretches from latitude 35.22 to 34.99 north to longitude 3.52 to 3.77 west. The Oued Amakran is the mainstream of the basin, its length was estimated to be 40 km and it flows into the Mediterranean Sea. The altitude of the study area ranges from 49 to 1,612 m, and its slope extends from 0 to 63°.
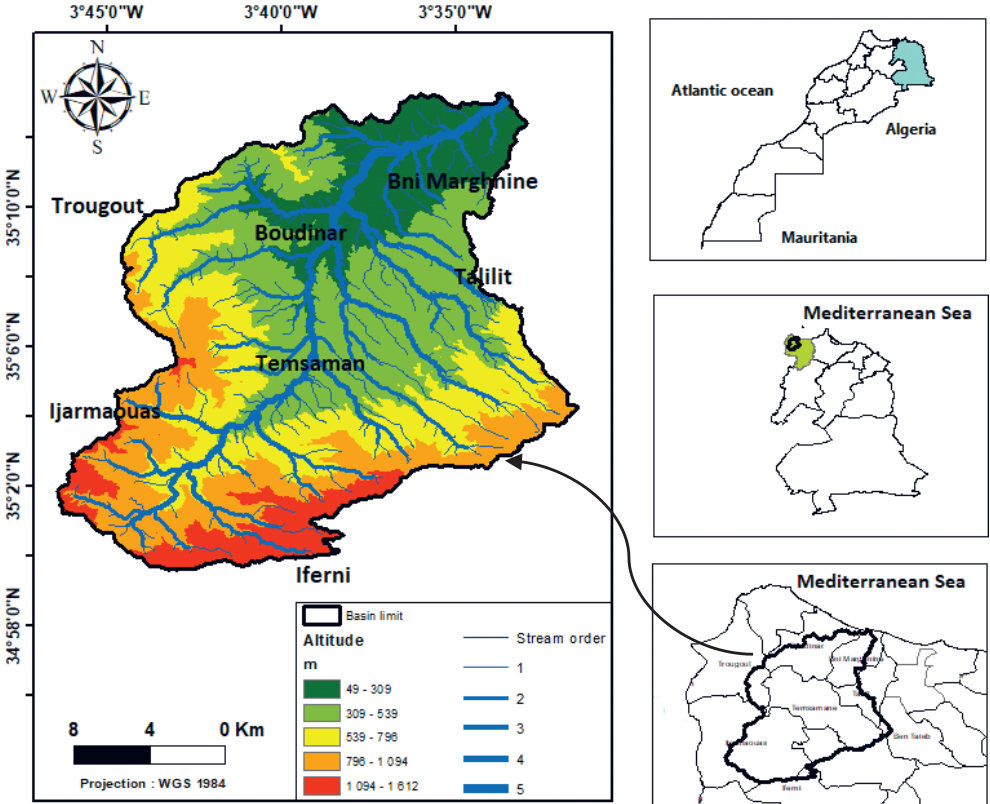


**Fig. 1.** The Geographical and administrative location of the Boudinar Basin

Geologically, the Boudinar Basin is located on the internal border of the Riffian chain [30]. It belongs to the post-nappe Neogene basins formed after the main orogenic movements of the Rif [31]. It includes distinct geological domains that range from the Jurassic to the Quaternary (Fig. 2). Based on the geological map of Boudinar, the basin is bordered to the west by andesitic terminal breccia of Neogene volcanics of the Ras-Tarf massif, and the Albo-Aptian sericite schist of the Ketama unit, to the east by the Taliouine pleated zone and the Sidi Messaoud unit, to the south by the Tafersit-Iferni zone. The sedimentary record of the Boudinar Basin is traditionally subdivided into three main series [31]: the Upper Tortonian sedimentary series, the Messinian series and the lower Pliocene series [30].
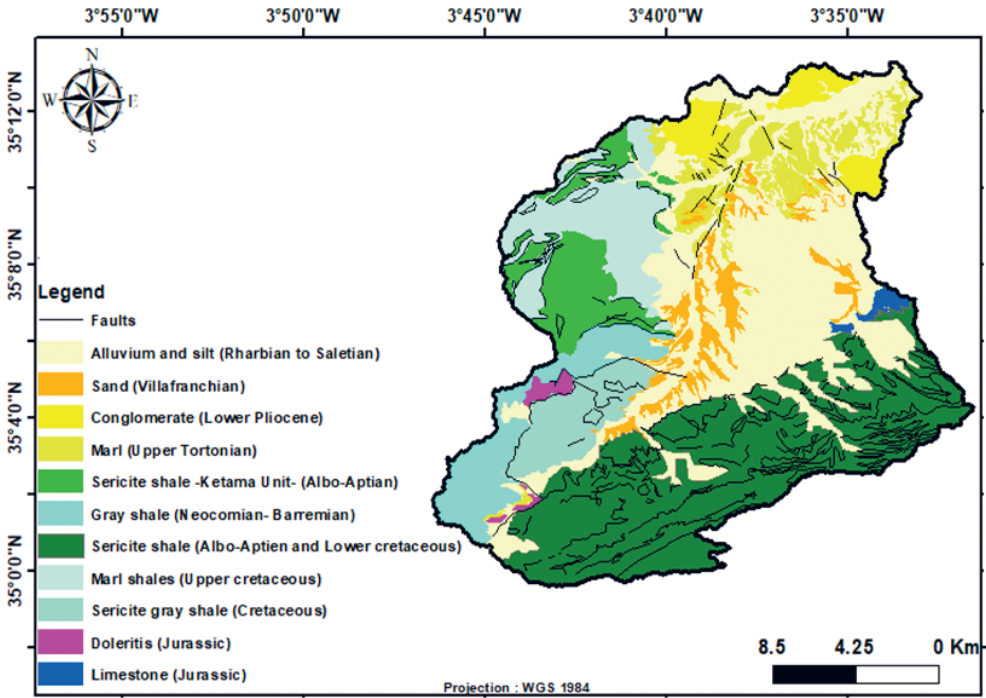
**Fig. 2.** The geological map of the Boudinar Basin

The annual precipitation (12 years) in the Boudinar Basin ranges between 394 and 441 mm, decreasing gradually to the northeast. Recently, rainfall (Fig. 3a) has decreased, and the temperature (Fig. 3b) has increased, resulting in water scarcity in the basin. Consequently, groundwater has become the sole source of drinking water for the population and animals.
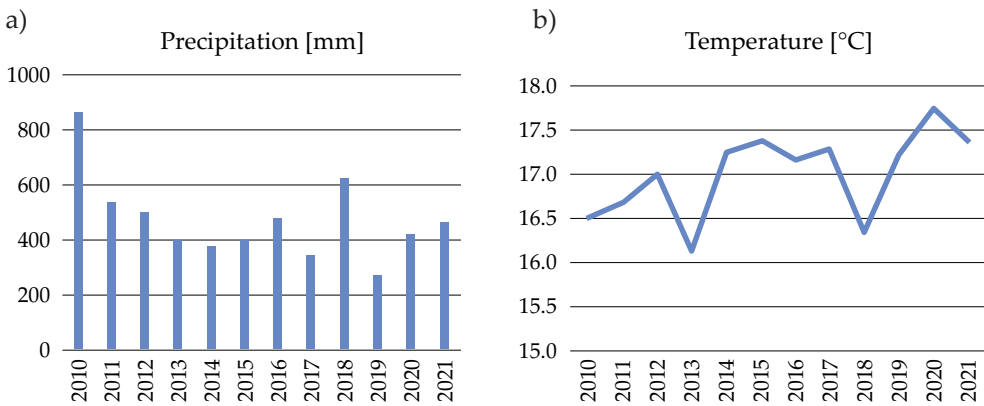


**Fig. 3.** Histogram of annual precipitation (a) and temperature (b)
of the Boudinar Basin (2010–2021)

According to the Moroccan High Commission for Planning (HCP), the Boudinar Basin total's populations in 2014 was 60,577: Boudinar 9,863, Beni Marghnine 6,223, Trougout 11,458, Temsamane 13,920, Talilit 5,208, Iferni 6,365, Ijermaouas 7,540 (Fig. 4). Additionally, the population increases during the summer.

Population/Commune
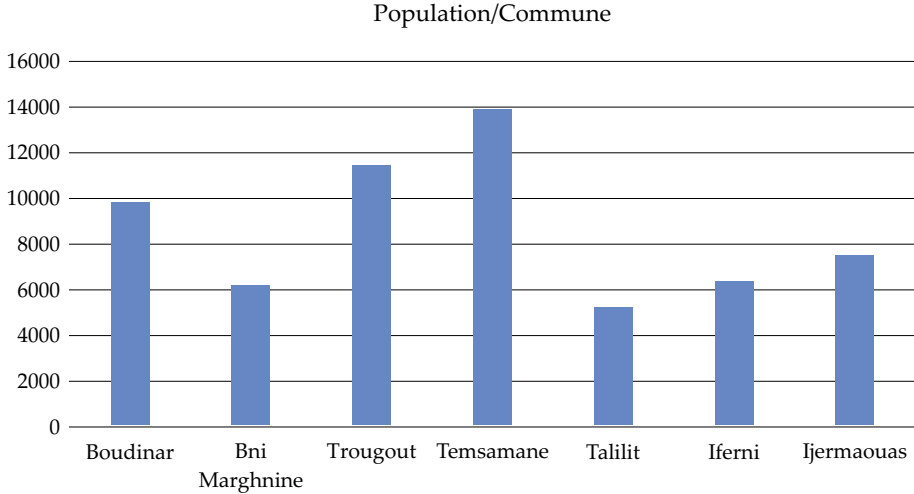


**Fig. 4.** Histogram of a population number per commune of the Boudinar Basin
Source: acc. to the HCP data (2014)

## 3.   Materials and Methods

### 3.1.  Data collection

The GWPZ map was very complex due to the shortage in data sets and a lot of calculation using 15 parameters. For the current study, the GWPZ map was generated using the data listed in Table 2. The NDVI and LULC maps were created using Landsat 9 OLI (30 × 30-meter pixels) satellite image (LC9_L2SP_200036_2022711_20220713_02_T1_SR) downloaded from the United States Geological Survey (USGS). The rainfall map was created using the inverse distance weighted (IDW) method based on data from the period 2010–2021 provided by NASA Langley Research Center (LaRC) POWER Project. The soil map was created using the soil classification map 1:50,000 (1994) of the provincial directorate of agriculture of Nador. The faults and the lithology maps were digitalized using the geological map of Boudinar 1:50,000 provided by the geological survey of Morocco. The topographic thematic layers (slope, TWI, elevation, roughness, curvature, drainage density) were extracted from the digital elevation model (DEM) (12.5 × 12.5-meter pixels), downloadable from the Earth Data (NASA) website. The 15 thematic maps were all reclassed using the weighted overlay analysis and the AHP technique. The methodology adopted in the current study is shown in Figure 5.

**Table 2.** Data sources

| Data | Source | Thematic layer |
|---|---|---|
| Landsat 9 OLI | USGS Earth Explorer | NDVI – LULC |
| Annual rainfall | POWER Project (NASA LaRC) | Rainfall |
| Soil data | Provincial directorate of agriculture of Nador | Soil |
| Geological map | Geological survey of Morocco | Lithology – Distance from fault – Lineament density |
| POLSAR (DEM) | Earth Data (NASA) | Altitude – Slope – TWI – Distance from river – Roughness – Plan curvature – Profile curvature – Drainage density |
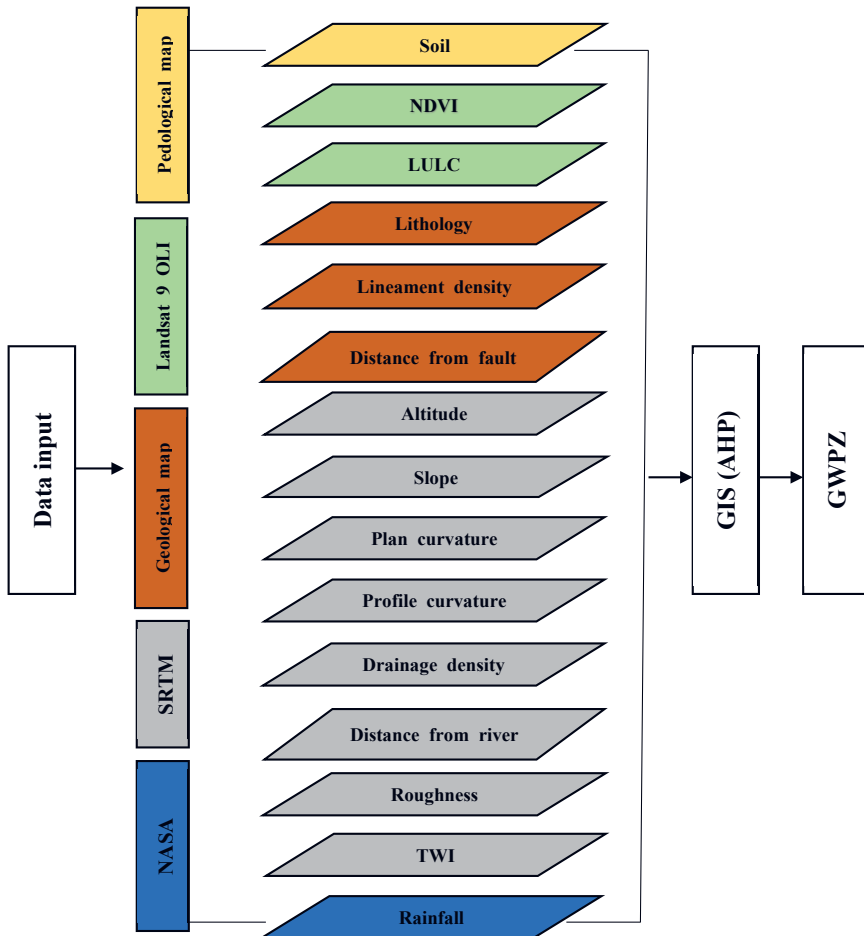


**Fig. 5.** Flow chart of the present study

### 3.2.  Analytical Hierarchy Process (AHP) Technique

The AHP is a tool of information communication and signification [32]. This method has proven its efficiency in decision-making [33]. The AHP is used widely by many searchers worldwide [14, 32–37].

**Table 3.** The fundamental scale

| Intensity | 1 | 3 | 5 | 7 | 9 |
|---|---|---|---|---|---|
| Definition | equal importance | moderate importance | strong importance | very strong importance | extreme importance |

2, 4, 6, 8 – intermediate values between the two adjacent judgments.

Source: [32]

**Table 4.** The random index (RI) value

| N | 1 | 2 | 3 | 4 | 5 | 6 | 7 | 8 | 9 |
|---|---|---|---|---|---|---|---|---|---|
| RI | 0.00 | 0.00 | 0.58 | 0.89 | 1.12 | 1.25 | 1.32 | 1.40 | 1.45 |

Source: [32]

The steps of the AHP technique are shown in Tables 3–6. The initial phase is the selection of essential criteria, which are compared using Saaty's scale (Tab. 3) [9]. The second step is computing the normalized weights (NW) (Tabs. 5, 6). The consistency ratio (CR) is calculated using the random index scale as the final step in the AHP [32] (Tab. 4):

$$CR = \frac{CI}{RCI},$$

$$CR = \frac{0.1347}{1.4} = 0.0962 < 0.1,$$

where:
CRI – random consistency index,
CI – consistency index,

$$CI = \frac{\lambda_{max} - n}{n-1} = \frac{16.8865 - 15}{15 - 1} = 0.13475,$$

where:
$\lambda_{max}$ – the principal eigenvalue ($\lambda_{max}$ = 16.8865),
$n$ – the number of factors.

**Table 5.** Pair-wise comparison matrix (explanations of abbreviations and acronyms as in Table 6)

| Rank | Factor | Alt | DFF | DFR | DD | LD | Lith | LULC | NDVI | PC | PrC | Rai | Roug | Slp | Soil | TWI | CW | Ratio |
|---|---|---|---|---|---|---|---|---|---|---|---|---|---|---|---|---|---|---|
| 3 | Alt | 1 | 1 | 1 | 3/4 | 3/5 | 3/8 | 3/7 | 3/6 | 3/1 | 3/1 | 3/6 | 3/1 | 3/3 | 3/5 | 3/4 | 0.0456 | 18.7719 |
| 2 | DFF | 2/3 | 1 | 1 | 2/4 | 2/5 | 2/8 | 2/7 | 2/6 | 2/1 | 2/1 | 2/6 | 2/1 | 2/3 | 2/5 | 2/4 | 0.0882 | 4.8175 |
| 2 | DFR | 2/3 | 1 | 1 | 2/4 | 2/5 | 2/8 | 2/7 | 2/6 | 2/1 | 2/1 | 2/6 | 2/1 | 2/3 | 2/5 | 2/4 | 0.0882 | 4.8175 |
| 4 | DD | 4/3 | 4/2 | 4/2 | 1 | 4/5 | 4/8 | 4/7 | 4/6 | 4/1 | 4/1 | 4/6 | 4/1 | 4/3 | 4/5 | 4/4 | 0.0609 | 18.7422 |
| 5 | LD | 5/3 | 5/2 | 5/2 | 5/4 | 1 | 5/8 | 5/7 | 5/6 | 5/1 | 5/1 | 5/6 | 5/1 | 5/3 | 5/5 | 5/4 | 0.0761 | 18.7451 |
| 8 | Lith | 8/3 | 8/2 | 8/2 | 8/4 | 8/5 | 1 | 8/7 | 8/6 | 8/1 | 8/1 | 8/6 | 8/1 | 8/3 | 8/5 | 8/4 | 0.1220 | 18.7279 |
| 7 | LULC | 7/3 | 7/2 | 7/2 | 7/4 | 7/5 | 7/8 | 1 | 7/6 | 7/1 | 7/1 | 7/6 | 7/1 | 7/1 | 7/5 | 7/4 | 0.1067 | 18.7263 |
| 6 | NDVI | 6/3 | 6/2 | 6/2 | 6/4 | 6/5 | 6/8 | 6/7 | 1 | 6/1 | 6/1 | 6/6 | 6/1 | 6/3 | 6/5 | 6/4 | 0.0915 | 18.7322 |
| 1 | PC | 1/3 | 1/2 | 1/2 | 1/4 | 1/5 | 1/8 | 1/7 | 1/6 | 1 | 1 | 1/6 | 1/1 | 1/3 | 1/5 | 1/4 | 0.0151 | 18.7417 |
| 1 | PrC | 1/3 | 1/2 | 1/2 | 1/4 | 1/5 | 1/8 | 1/7 | 1/6 | 1 | 1 | 1/6 | 1/1 | 1/3 | 1/5 | 1/4 | 0.0151 | 18.7417 |
| 6 | Rai | 6/3 | 6/2 | 6/2 | 6/4 | 6/5 | 6/8 | 6/7 | 6/6 | 6/1 | 6/1 | 1 | 6/1 | 6/3 | 6/5 | 6/4 | 0.0915 | 18.7322 |
| 1 | Roug | 1/3 | 1/2 | 1/2 | 1/4 | 1/5 | 1/8 | 1/7 | 1/6 | 1/1 | 1/1 | 1/6 | 1 | 1/3 | 1/5 | 1/4 | 0.0151 | 18.7417 |
| 3 | Slp | 3/3 | 3/2 | 3/2 | 3/4 | 3/5 | 3/8 | 3/7 | 3/6 | 3/1 | 3/1 | 3/6 | 3/1 | 1 | 3/5 | 3/4 | 0.0456 | 18.7719 |
| 5 | Soil | 5/3 | 5/2 | 5/2 | 5/4 | 5/5 | 5/8 | 5/7 | 5/6 | 5/1 | 5/1 | 5/6 | 5/1 | 5/3 | 1 | 5/4 | 0.0761 | 18.7451 |
| 4 | TWI | 4/3 | 4/2 | 4/2 | 4/4 | 4/5 | 4/8 | 4/7 | 4/6 | 4/1 | 4/1 | 4/6 | 4/1 | 4/3 | 4/5 | 1 | 0.0609 | 18.7422 |

**Table 6.** Normalized Layer Weight (NW) of subclasses

| Influencing factors | Class interval | Reclass | Overlay | Rank | NW | NW% |
|---|---|---|---|---|---|---|
| Altitude (Alt) | 49 – 309<br>309 – 539<br>539 – 796<br>796 – 1094<br>1094 – 1612 | 1<br>2<br>3<br>4<br>5 | 5<br>4<br>3<br>2<br>1 | 3 | 0.0456 | 4 |
| Distance from fault (DFF) | 0.000 – 0.011<br>0.011 – 0.020<br>0.020 – 0.030<br>0.030 – 0.040<br>0.040 – 0.052 | 1<br>2<br>3<br>4<br>5 | 5<br>4<br>3<br>2<br>1 | 2 | 0.0882 | 8 |
| Distance from river (DFR) | 0.0 – 218<br>218 – 437<br>437 – 656<br>656 – 874<br>874 – 1093 | 1<br>2<br>3<br>4<br>5 | 5<br>4<br>3<br>2<br>1 | 2 | 0.0882 | 8 |
| Drainage density (DD) | 0.00 – 0.58<br>0.58 – 1.17<br>1.17 – 1.76<br>1.76 – 2.34<br>2.34 – 2.93 | 1<br>2<br>3<br>4<br>5 | 5<br>4<br>3<br>2<br>1 | 4 | 0.0609 | 6 |
| Lineament density (LD) | 0.00 – 40.78<br>40.78 – 81.56<br>81.56 – 122.34<br>122.34 – 163.12<br>163.12 – 203.90 | 1<br>2<br>3<br>4<br>5 | 1<br>2<br>3<br>4<br>5 | 5 | 0.0761 | 7 |
| Lithology (Lith) | Alluvium and silt<br>Conglomerate<br>Dolerites<br>Limestone<br>Marl<br>Sand<br>Sericite gray shale | –<br>–<br>–<br>–<br>–<br>–<br>– | 5<br>1<br>1<br>3<br>4<br>5<br>3 | 8 | 0.1220 | 12 |
| LULC | Vegetation<br>Bare ground | –<br>– | 3<br>1 | 7 | 0.1067 | 11 |
| NDVI | −0.06 – 0.0940<br>0.0941 – 0.1270<br>0.1271 – 0.1660<br>0.1661 – 0.2210<br>0.2211 – 0.4557 | 1<br>2<br>3<br>4<br>5 | 1<br>2<br>3<br>4<br>5 | 6 | 0.0915 | 10 |

**Table 6.** cont.

| | | | | | | |
|---|---|---|---|---|---|---|
| Plan curvature (PC) | −11.00 – −1.04<br>−1.03 – −0.40<br>−0.40 – 0.23<br>0.23 – 0.88<br>0.88 – 6.94 | 1<br>2<br>3<br>4<br>5 | 1<br>2<br>3<br>4<br>5 | 1 | 0.0151 | 2 |
| Profile curvature (PrC) | −6.96 – −1.01<br>−1.00 – −0.39<br>−0.39 – 0.21<br>0.21 – 0.90<br>0.90 – 10.75 | 1<br>2<br>3<br>4<br>5 | 1<br>2<br>3<br>4<br>5 | 1 | 0.0151 | 2 |
| Rainfall (Rai) | 394.42 – 403.79<br>403.79 – 413.16<br>413.16 – 422.53<br>422.53 – 431.90<br>431.90 – 441.27 | 1<br>2<br>3<br>4<br>5 | 1<br>2<br>3<br>4<br>5 | 6 | 0.0915 | 10 |
| Roughness (Roug) | 0.11 – 0.32<br>0.32 – 0.45<br>0.45 – 0.53<br>0.53 – 0.67<br>0.67 – 0.89 | 1<br>2<br>3<br>4<br>5 | 5<br>4<br>3<br>2<br>1 | 1 | 0.0151 | 2 |
| Slope (Slp) | 0.00 – 7.97<br>7.97 – 14.45<br>14.45 – 20.68<br>20.86 – 28.16<br>28.16 – 63.56 | 1<br>2<br>3<br>4<br>5 | 5<br>4<br>3<br>2<br>1 | 3 | 0.0456 | 5 |
| Soil | I<br>II<br>III<br>V<br>V+ | –<br>–<br>–<br>–<br>– | 1<br>2<br>3<br>4<br>5 | 5 | 0.0761 | 7 |
| TWI | 2.12 – 4.87<br>4.87 – 6.42<br>6.42 – 8.57<br>8.57 – 12.35<br>12.35 – 24.05 | 1<br>2<br>3<br>4<br>5 | 1<br>2<br>3<br>4<br>5 | 4 | 0.0609 | 6 |

### 3.3. Factors Influencing Groundwater

To accurately delineate the GWPZ, choosing the appropriate technique and factors to include is a critical stage. Hence, based on the literature review of studies dealing with GWPZ delineation (Tab. 7), fifteen groundwater influential factors

were chosen: lithology, slope, TWI, plan curvature, profile curvature, NDVI, LULC, lineament density, drainage density, altitude, distance from fault, distance from river, soil, roughness, and rainfall (Fig. 6 on the interleaf). The combination of thematic layers of these factors led to the identification of the GWPZ. It is worth indicating that the consistency ratio (CR) should be less than 0.1 to consider the weights affected logically by the factors.

**Table 7.** A summary of factors employed to delineate GWPZ
based on the literature review

| Parameter | The authors used the same parameter |
|---|---|
| Elevation (altitude) | [35], [38], [39] |
| Soil | [39], [40], [41] |
| Distance from fault | [3] |
| Distance from river | [3] |
| Drainage density | [9], [33], [41] |
| Lineament density | [23], [27], [40] |
| Lithology | [33], [35], [39] |
| LULC | [23], [26], [33] |
| NDVI | [3], [14], [33] |
| Profile curvature | [3], [10] |
| Plan curvature | [3], [10] |
| Rainfall | [7], [14], [39] |
| Roughness | [14] |
| Slope | [14], [35], [38] |
| TWI | [3], [10], [35] |

### 3.4.  Groundwater Potential Parameters

**Rainfall, elevation (altitude) and slope**

Rainfall distribution is an essential parameter in identifying GWPZ [27]. Due to the challenges in acquiring reliable local rainfall data, we used the rainfall data of NASA as mentioned above in the materials and method section. Based on the annual rainfall map (2010–2021) in Figure 6k, the Boudinar Basin rainfall ranges between 394 and 441 mm and decreases from the south (high elevation) to the north (low elevation). The higher rainfall areas were more favorable for groundwater (high weights) recharge than lower rainfall areas (low weights) (Tab. 6).

Elevation (altitude) is a key feature in determining the infiltration rate of the rainfall [38, 39]. The lower elevation (higher weights) areas were more favorable for groundwater recharge predictions than higher elevations (lower weights) [35] (Tab. 6). According to the elevation map (Fig. 6a), the altitude varies from 49 to 1612 m.

The slope of an area is an essential parameter in identifying GWPZ [10, 23, 26], it determines the rate of infiltration and runoff of surface water [10, 38]. High-degree slopes increase the runoff and decrease the infiltration (lower weights), whereas the low-degree slope and flat surface facilitate groundwater recharge (higher weights) (Tab. 6) [26]. The slope gradients in the Boudinar Basin (Fig. 6n) range between 0 and 63°. The low gradient slope is concentrated in the middle east and northeast of the basin. The high gradient slope is noticed in the south, southwest, and southeast of the basin.

**Soil, lithology, NDVI and LULC**

Soils texture plays a crucial role in water transport (vertical and horizontal) [40]. According to the soil map classification, the soil map of the study area (Fig. 6b) revealed five soil texture classes, ranging from the fine texture (low weights) to coarse texture (high weights) (Tab. 6).

Lithology is highly recommended for GWPZ to assess groundwater porosity and movement [33]. The lithological map (Fig. 6g) of the study area contained three principal types: alluvium, silt, and sand (very higher weights) in the middle and in the northeast of the district, sericite gray shale (medium weights) in the south, southeast and southwest, finally, marl in the north and northwest (high weights) (Tab. 6).

Both NDVI and LULC were equally important in GWPZ delineation, as they provide essential information on infiltration [26]. The NDVI (Fig. 6i) and LULC (Fig. 6h) maps show that higher rates of vegetation are in the middle west and the south of the study area. The NDVI value range between −0.06 and 0.45, negative values indicate no vegetation cover and vice versa [33]. For the potential groundwater areas, higher NDVI values were given higher weights, and vice versa [42] (Tab. 6).

**Distance from fault and distance from river**

The distance from faults map (Fig. 6c) was generated using the faults map, digitized from the geological map of Boudinar at a 1:50,000 scale. The distance from faults map was used to infer groundwater storage because groundwater flow direction is

controlled by fault systems [3]. Furthermore, rivers are one of the sources of ground-water, and thus they influence groundwater potential in a watershed [3]. The distance from river map (Fig. 6d) was generated from the stream map. The Euclidean distance tool was used to create distance categories. The two distance maps were reclassified into five classes, the high value was assigned a lower weight, and vice versa (Tab. 6). Generally, these two factors are rarely used by researchers.

### Drainage density and lineament density

Drainage density is a key indicator of surface infiltration rate and surface run-off [33, 40]. The drainage density map (Fig. 6e) was categorized into five classes, its value ranges between 0 and 2.93 km/km$^2$. The high values indicate low groundwater availability and were assigned a low weight and vice versa.

Lineaments such as faulting and fracturing in the subsurface are responsible for groundwater occurrence [15, 31]. Therefore, this factor is considered one of the most significant characteristics for observing GWPZ [42]. The lineaments density map values (Fig. 6f) of the Boudinar Basin range from 0 to 203 km/km$^2$. The values were reclassified into five categories. The high weightage was assigned to a higher value of lineament density, and vice versa (Tab. 6).

### Profile curvature and plan curvature

Flow distribution on the surface depends on topography, which is represented by profile and plan curvature [3]. The profile curvature, which is parallel to the direction of the maximum slope, affects the acceleration of water flows at the basin [10]. The profile curvature map (Fig. 6j) of the study area was classified into five classes. Its values range between −6.69 to 10.75. A negative-positive value indicates that the surface is convex and concave consecutively upward on this cell, while a zero indicates linear surface. Plan curvature mainly affects flow convergence and divergence [3]. Its related map (Fig. 6l) was also categorized into five classes. Its values range between −11 and 6.94, positive and negative values indicate that the surface is convex and concave consecutively laterally to this cell, while a zero value indicates a linear surface [43]. For the two maps, a high weightage was assigned a higher value, and vice versa (Tab. 6).

### Roughness and TWI

Surface roughness is a critical parameter for GWPZ. It was used in different ways to indicate the variation of surface property [44]. The roughness map (Fig. 6m) was categorized into five classes and its values range between 0.11 to 0.89. High weights were allocated to low values of roughness, and vice versa [15].

The topographic wetness index (TWI) is used to quantify the effect of topographic and hydrological processes [10, 33] and is therefore an important parameter to identify the GWPZ. The TWI is calculated using the following equation: TWI = ln (As/tanβ), where As is flow accumulation, and β is slope gradient [43]. The TWI values (Fig. 6o) in the study area range from 2.12 to 24.05. It was classified into five classes. The high value was given a high weight and vice versa (Tab. 6).

## 4. Results

The delineation of the GWPZ in the Boudinar Basin was achieved using the AHP method and geospatial (RS and GIS) techniques. All the following 15 parameters were integrated: altitude, slope, lithology, lineament density, drainage density, etc. All these thematic layers were converted to a raster format in a GIS environment. Furthermore, the rank value (Tab. 6) was assigned to each parameter regarding their importance in groundwater occurrence.

The standard AHP procedures were followed to derive the weights of the thematic layers and to calculate the consistency ratio (CR), which in the present study equals to 9% CR < 10%, reflecting a good level of consistency in the pair-wise comparison phase.

The obtained groundwater potential map (Fig. 7) depicts three zone classes:
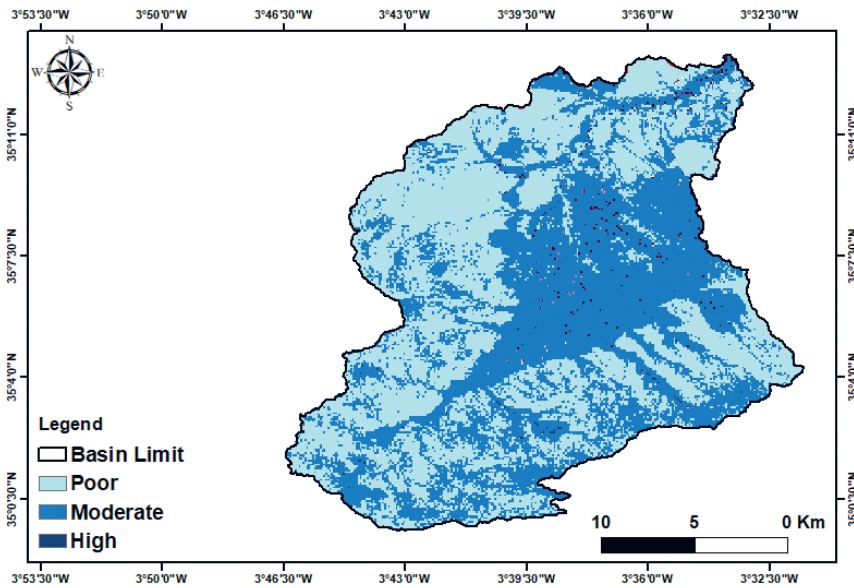1) high (<1%),
2) moderate (50.82%),
3) poor (49.06%).



**Fig. 7.** The groundwater potential zone of the Boudinar Basin

The result shows that high and moderate GWPZs occur the middle east of the study area, where the area is covered with alluvial and sand deposits, areas with low slope gradient, and high TWI. Furthermore, poor GWPZs were identified in the southern and southwestern parts of the Boudinar Basin. It is covered by sericite gray shale, a high slope gradient, a high elevation, and a low TWI.

## 5. Discussion

The validation of results is an essential step in any predictive modeling in order to have scientific significance [25, 26, 45]. For the validation of GWPZ, various methods have been widely used, such as receiver performance analysis (ROC), and curve area (AUC) [9, 18, 23, 37]. Therefore, many researchers conducted a field survey to determine the wells' water table depth or their yield to validate their result [28, 42]. According to our survey, the water depth of 15 wells ranged from a low of 9 m to a high of 103 m (Fig. 8). Unfortunately, due to the precipitation scarcity in recent years and the concomitant overuse of groundwater in the Boudinar Basin, the water depth of wells in the study area increased and made it impossible to apply the level classification of the previous studies for calculating the AUC [18, 26, 40].

In this context, to compare the result obtained in the GWPZ map (Fig. 7), we adopted four other different scenarios used in the selected literature review to delineate the GWPZ in the Boudinar Basin (Tab. 8).

The result of the GWPZ map of the four scenarios are (Fig. 9):
- scenario 1: poor 42%, moderate 57%, good <1%,
- scenario 2: poor 47%, moderate 52%, good <1%,
- scenario 3: poor 26%, moderate 53%, good 20%,
- scenario 4: poor 17%, moderate 80%, good 2%.

Therefore, the first and the second scenarios are the most similar result obtained using the 15 parameters. However, it must be noted that the uncertainties regarding LULC and climate data may have impacted the GWPZ maps.
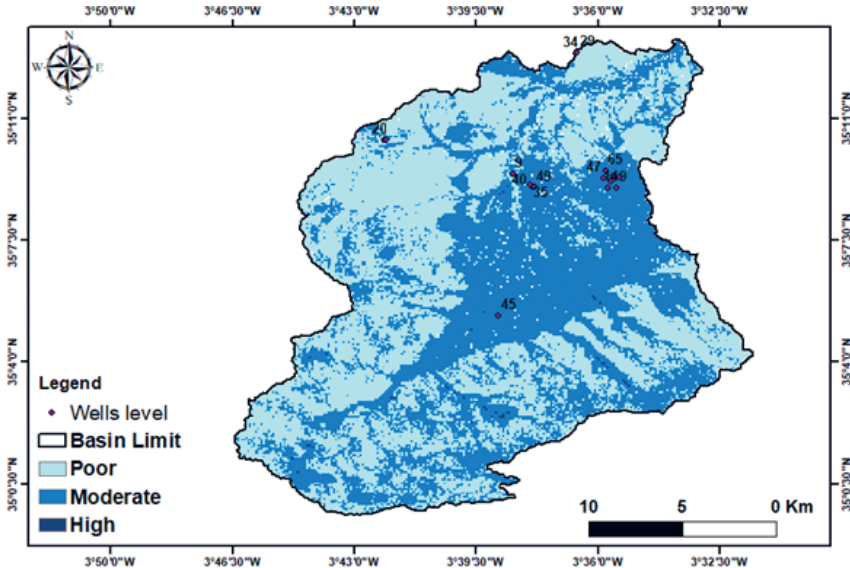


**Fig. 8.** Groundwater potential map of the study area with well depth

**Table 8.** The four scenarios of GWPZ for Boudinar Basin

| Scenario | Parameters | Weight [%] | Authors |
|---|---|---|---|
| 1 | Lithology<br>Lineament density<br>Slope<br>LULC<br>Drainage density<br>Rainfall | 19<br>19<br>14<br>24<br>14<br>10 | [46] |
| 2 | Lithology<br>Lineament density<br>Slope<br>LULC<br>Drainage density<br>Soil | 15<br>30<br>20<br>10<br>10<br>15 | [47] |
| 3 | Lithology<br>Slope<br>Lineament density<br>Soil<br>Elevation (altitude)<br>Drainage density<br>LULC | 38<br>19<br>13<br>10<br>8<br>6<br>6 | [38] |
| 4 | Lithology<br>Lineament density<br>Drainage density<br>Slope<br>Rainfall | 30<br>30<br>15<br>10<br>15 | [7] |
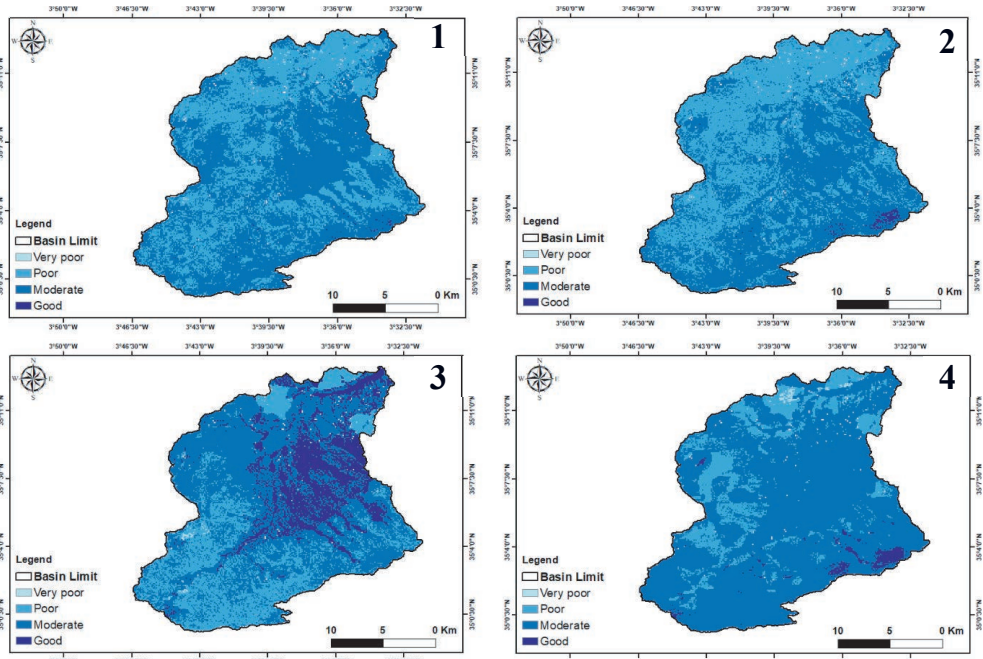


**Fig. 9.** The GWPZ maps of the four scenarios

## 6. Conclusion

The GWPZs of the Boudinar Basin, a rural coastal region, were delineated for the first time using remote sensing and GIS techniques. Furthermore, the analytical hierarchy process method was used for GWPZ delineation due to its efficiency. Accordingly, 15 selected parameters were prepared and assigned weights according to their influence on groundwater occurrence. The GWPZ map of the study area indicates that the majority of the district is covered by a mo preliminary reference for selecting suitable sites for drilling new boreholes to cope with water scarcity in the future and to encourage socio-economic activities that are related to water, such as agriculture and tourism. The Boudinar Basin requires further hydrogeological studies, either modeling studies (GWPZ, marine intrusion) or fieldwork studies (hydrogeochemical and isotopic). Finally, this approach can be used in any similar area in Morocco and worldwide.

## References

[1] Díaz-Alcaide S., Martínez-Santos P.: *Review: Advances in groundwater potential mapping*. Hydrogeology Journal, vol. 27(7), 2019, pp. 2307–2324. https://doi.org/10.1007/s10040-019-02001-3.

[2] Hasanuzzaman M., Mandal M.H., Hasnine M., Shit P.K.: *Groundwater potential mapping using multi – criteria decision, bivariate statistic and machine learning algorithms: evidence from Chota Nagpur Plateau, India*. Applied Water Science, vol. 12(4), 2022, pp. 1–16. https://doi.org/10.1007/s13201-022-01584-9.

[3] Jaafarzadeh M.S., Tahmasebipour N., Haghizadeh A., Pourghasemi H.R., Rouhani H.: *Groundwater recharge potential zonation using an ensemble of machine learning and bivariate statistical models*. Scientific Reports, vol. 11, 2021, 5587. https://doi.org/10.1038/s41598-021-85205-6.

[4] Endalamaw N.T., Moges M.A., Kebede Y.S., Alehegn B.M., Sinshaw B.G.: *Potential soil loss estimation for conservation planning, upper Blue Nile Basin, Ethiopia*. Environmental Challenges, vol. 5, 2021, 100224. https://doi.org/10.1016/j.envc.2021.100224.

[5] Gómez-Escalonilla V., Martínez-Santos P., Martín-Loeches M.: *Preprocessing approaches in machine-learning-based groundwater potential mapping: an application to the Koulikoro and Bamako regions, Mali*. Hydrology and Earth System Sciences, vol. 26(2), 2022, pp. 221–243. https://doi.org/10.5194/hess-26-221-2022.

[6] Khan M.Y.A., Elkashouty M., Tian F.: *Mapping groundwater potential zones using analytical hierarchical process and multicriteria evaluation in the Central Eastern*

*Desert, Egypt.* Water (Switzerland), vol. 14(7), 2022, 1041. https://doi.org/10.3390/w14071041.

[7] Saadi O., Nouayti N., Nouayti A., Dimane F., Elhairechi K.: *Application of remote sensing data and geographic information system for identifying potential areas of groundwater storage in middle Moulouya Basin of Morocco.* Groundwater for Sustainable Development, vol. 14, 2021, 100639. https://doi.org/10.1016/j.gsd.2021.100639.

[8] Nouayti A., Khattach D., Hilali M., Nouayti N.: *Mapping potential areas for groundwater storage in the high Guir Basin (Morocco): Contribution of remote sensing and geographic information system.* Journal of Groundwater Science and Engineering, vol. 7(4), 2019, pp. 309–322. https://doi.org/10.19637/j.cnki.2305-7068.2019.04.002.

[9] Ifediegwu S.I.: *Assessment of groundwater potential zones using GIS and AHP techniques: A case study of the Lafia district, Nasarawa State, Nigeria.* Applied Water Science, vol. 12(1), 2022, 10. https://doi.org/10.1007/s13201-021-01556-5.

[10] Echogdali F.Z., Boutaleb S., Kpan R.B., Ouchchen M., Bendarma A., El Ayady H., Abdelrahman K. et al.: *Application of fuzzy logic and fractal modeling approach for groundwater potential mapping in Semi-Arid Akka Basin, Southeast Morocco.* Sustainability, vol. 14(16), 2022, 10205. https://doi.org/10.3390/su141610205.

[11] Mall R.K., Gupta A., Singh R., Singh R.S., Rathore L.S.: *Water resources and climate change: An Indian perspective.* Current Science, vol. 90(12), 2006, pp. 1610–1626.

[12] Aouragh M.H., Essahlaoui A., El Ouali A., El Hmaidi A., Kamel S.: *Groundwater potential of Middle Atlas plateaus, Morocco, using fuzzy logic approach, GIS and remote sensing.* Geomatics, Natural Hazards and Risk, vol. 8(2), 2017, pp. 194–206. https://doi.org/10.1080/19475705.2016.1181676.

[13] Taher M., Mourabit T., Bourjila A., Saadi O., Errahmouni A., El Marzkioui F., El Mousaoui M.: *An estimation of soil erosion rate hot spots by integrated USLE and GIS methods: A case study of the Ghiss Dam and Basin in Northeastern Morocco.* Geomatics and Environmental Engineering, vol. 16(2), pp. 95–110, 2022. https://doi.org/10.7494/geom.2022.16.2.95.

[14] Bourjila A., Dimane F., El Ouarghi H., Nouayti N., Taher M.: *Groundwater potential zones mapping by applying GIS, remote sensing and multi-criteria decision analysis in the Ghiss basin, northern Morocco.* Groundwater for Sustainable Development, vol. 15, 2021, 100693. https://doi.org/10.1016/j.gsd.2021.100693.

[15] Bourjila A., Dimane F., Nouayti N., Taher M., El Ouarghi H.: *Use of GIS, remote sensing and AHP techniques to delineate groundwater potential zones in the Nekor Basin, Central Rif of Morocco.* [in:] *GEOIT4W-2020: Proceedings of the 4th Edition of International Conference on Geo-IT and Water Resources 2020, Geo-IT and Water Resources 2020,* Association for Computing Machinery, New York 2020, pp. 1–7. https://doi.org/10.1145/3399205.3399219.

[16] Errahmouni A., Stitou El Messari J.E., Taher M.: *Estimation of groundwater recharge using APLIS method – case study of Bokoya Massif (Central Rif, Morocco)*. Ecological Engineering & Environmental Technology, vol. 23(4), 2022, pp. 57–66. https://doi.org/10.12912/27197050/149956.

[17] Al-Gburi M.R.G., Al-Khatony S.E., Znad R.Kh., Al-Sumaidaie M.A.H.: *Mapping of groundwater potential zone using GIS and remote sensing of Shwan Sub-Basin, Kirkuk, NE Iraq*. Iraqi Geological Journal, vol. 55(2B), 2022, pp. 62–72. https://doi.org/10.46717/igj.55.2B.6Ms-2022-08-22.

[18] Kumar M., Singh P., Singh P.: *Fuzzy AHP based GIS and remote sensing techniques for the groundwater potential zonation for Bundelkhand Craton Region, India*. Geocarto International, vol. 37(22), 2022, pp. 6671–6694. https://doi.org/10.1080/10106049.2021.1946170.

[19] Masoud A.M., Pham Q.B., Alezabawy A.K., Abu El-Magd S.A.: *Efficiency of geospatial technology and multi-criteria decision analysis for groundwater potential mapping in a Semi-Arid Region*. Water (Switzerland), vol. 14(6), 2022, 882. https://doi.org/10.3390/w14060882.

[20] Zhu Q., Abdelkareem M.: *Mapping groundwater potential zones using a knowledge-driven approach and GIS analysis*. Water(Switzerland), vol. 13(5), 2021, 579. https://doi.org/10.3390/w13050579.

[21] Khan M.Y.A., ElKashouty M., Subyani A.M., Tian F., Gusti W.: *GIS and RS intelligence in delineating the groundwater potential zones in Arid Regions: A case study of southern Aseer, southwestern Saudi Arabia*. Applied Water Science, vol. 12(1), 2022, 3. https://doi.org/10.1007/s13201-021-01535-w.

[22] Elvis B.W.W., Arsène M., Théophile N.M., Bruno K.M.E., Olivier O.A.: *Integration of shannon entropy (SE), frequency ratio (FR) and analytical hierarchy process (AHP) in GIS for suitable groundwater potential zones targeting in the Yoyo river basin, Méiganga area, Adamawa Cameroon*. Journal of Hydrology: Regional Studies, vol. 39, 2022, 100997. https://doi.org/10.1016/j.ejrh.2022.100997.

[23] Moodley T., Seyam M., Abunama T., Bux F.: *Delineation of groundwater potential zones in KwaZulu-Natal, South Africa using remote sensing, GIS and AHP*. Journal of African Earth Sciences, vol. 193, 2022, 104571. https://doi.org/10.1016/j.jafrearsci.2022.104571.

[24] Ahmadi H., Kaya O.A., Babadagi E., Savas T., Pekkan E.: *GIS-based groundwater potentiality mapping using AHP and FR models in Central Antalya, Turkey*. Environmental Sciences Proceedings, vol. 5(1), 2021, 11. https://doi.org/10.3390/IECG2020-08741.

[25] Melese T., Belay T.: *Groundwater potential zone mapping using analytical hierarchy process and GIS in Muga Watershed, Abay Basin, Ethiopia*. Global Challenges, vol. 6(1), 2022, 2100068. https://doi.org/10.1002/gch2.202100068.

[26] Pathmanandakumar V., Thasarathan N., Ranagalage M.: *An approach to delineate potential groundwater zones in Kilinochchi district, Sri Lanka, using GIS*

*techniques*. ISPRS International Journal of Geo-Information, vol. 10(11), 2021, 730. https://doi.org/10.3390/ijgi10110730.

[27] Dar T., Rai N., Bhat A.: *Delineation of potential groundwater recharge zones using analytical hierarchy process (AHP)*. Geology, Ecology, and Landscapes, vol. 5(4), 2021, pp. 292–307. https://doi.org/10.1080/24749508.2020.1726562.

[28] Nithya C.N., Srinivas Y., Magesh N.S., Kaliraj S.: *Assessment of groundwater potential zones in Chittar basin, Southern India using GIS based AHP technique*. Remote Sensing Applications: Society and Environment, vol. 15, 2019, 100248. https://doi.org/10.1016/j.rsase.2019.100248.

[29] Rajasekhar M., Sudarsana Raju G., Sreenivasulu Y., Siddi Raju R.: *Delineation of groundwater potential zones in semi-arid region of Jilledubanderu river basin, Anantapur District, Andhra Pradesh, India using fuzzy logic, AHP and integrated fuzzy-AHP approaches*. HydroResearch, vol. 2, 2019, pp. 97–108. https://doi.org/10.1016/j.hydres.2019.11.006.

[30] El Ouahabi F.Z., Saint Martin S., Saint Martin J.-P., Ben Moussa A., Conesa G.: *Les assemblages de diatomées du bassin messinien de Boudinar (Maroc nord-oriental). Messinian diatom assemblages from Boudinar basin (northeastern Rif, Morocco)*. Revue de Micropaléontologie, vol. 50(2), 2007, pp. 149–167. https://doi.org/10.1016/j.revmic.2007.02.004.

[31] Achalhi M., Münch Ph., Cornée J.-J., Azdimousa A., Melinte-Dobrinescu M., Quillévéré F., Drinia H. et al.: *The late Miocene Mediterranean-Atlantic connections through the North Rifian Corridor: New insights from the Boudinar and Arbaa Taourirt basins (northeastern Rif, Morocco)*. Palaeogeography, Palaeoclimatology, Palaeoecology, vol. 459, 2016, pp. 131–152. https://doi.org/10.1016/j.palaeo.2016.06.040.

[32] Saaty T.L.: *How to make a decision: The analytic hierarchy process*. European Journal of Operational Research, vol. 48(1), 1990, pp. 9–26. https://doi.org/10.1016/0377-2217(90)90057-I.

[33] Senapati U., Kumar Das T.: *GIS-based comparative assessment of groundwater potential zone using MIF and AHP techniques in Cooch Behar district, West Bengal*. Applied Water Science, vol. 12(3), 2022, 43. https://doi.org/10.1007/s13201-021-01509-y.

[34] Abdelouhed F., Ahmed A., Abdellah A., Yassine B., Mohammed I.: *Using GIS and remote sensing for the mapping of potential groundwater zones in fractured environments in the CHAOUIA-Morocco area*. Remote Sensing Applications: Society and Environment, vol. 23, 2021, 100571. https://doi.org/10.1016/j.rsase.2021.100571.

[35] Mengistu T.D., Chang S.W., Kim I.-H., Kim M.-G., Chung I.-M.: *Determination of potential aquifer recharge zones using geospatial techniques for proxy data of Gilgel Gibe Catchment, Ethiopia*. Water, vol. 14(9), 2022, 1362. https://doi.org/10.3390/w14091362.

[36] Mhaske S.N., Pathak K., Dash S.S., Nayak D.B.: *Assessment and management of soil erosion in the hilltop mining dominated catchment using GIS integrated RUSLE model*. Journal of Environmental Management, vol. 294, 2021, 112987. https://doi.org/10.1016/j.jenvman.2021.112987.

[37] Rajasekhar M., Upendra B., Raju G.S., Anand: *Identification of groundwater potential zones in southern India using geospatial and decision-making approaches*. Applied Water Science, vol. 12(4), 2022, 68. https://doi.org/10.1007/s13201-022-01603-9.

[38] Argaz A., Ouahman B., Darkaoui A., Bikhtar H., Yabsa K., Laghzal A.: *Application of remote sensing techniques and GIS-multicriteria decision analysis for groundwater potential mapping in Souss Watershed, Morocco*. Journal of Materials and Environmental Sciences, vol. 10(5), 2019, pp. 411–421.

[39] Rajesh J., Pande Ch.B., Kadam S.A., Gorantiwar S.D., Shinde M.G.: *Exploration of groundwater potential zones using analytical hierarchical process (AHP) approach in the Godavari river basin of Maharashtra in India*. Applied Water Science, vol. 11(12), 2021, 182. https://doi.org/10.1007/s13201-021-01518-x.

[40] Sarwar A., Ahmad S.R., Rehmani M.I.A., Asif Javid M., Gulzar S., Shehzad M.A., Shabbir Dar J. et al.: *Mapping groundwater potential for irrigation, by geographical information system and remote sensing techniques: A case study of district Lower Dir, Pakistan*. Atmosphere, vol. 12(6), 2021, 669. https://doi.org/10.3390/atmos12060669.

[41] Ghute B.B., Babar S.: *An approach to mapping groundwater recharge potential zones using geospatial techniques in Kayadhu River Basin, Maharashtra*. Indian Journal of Agricultural Research, vol. 55(1), 2021, pp. 23–32. https://doi.org/10.18805/IJARe.A-5477.

[42] Pande Ch.B., Moharir K.N., Panneerselvam B., Singh S.K., Elbeltagi A., Pham Q.B., Varade A.M., Rajesh J.: *Delineation of groundwater potential zones for sustainable development and planning using analytical hierarchy process (AHP), and MIF techniques*. Applied Water Science, vol. 11(12), 2021, 186. https://doi.org/10.1007/s13201-021-01522-1.

[43] Cole D.G. [review of the book *Map Use: Reading, Analysis, Interpretation, 8th Edition*, by A. Jon Kimerling, Aileen R. Buckley, Phillip C. Muehrcke, and Juliana O. Muehrcke; foreword by Jack Dangermond, ESRI Press 2016]. Cartographic Perspectives, no. 88, 2017, pp. 39–42.

[44] Habib M.: *Evaluation of DEM interpolation techniques for characterizing terrain roughness*. Catena, vol. 198, 2021, 105072. https://doi.org/10.1016/j.catena.2020.105072.

[45] Echogdali F.Z., Boutaleb S., Bendarma A., Saidi M.E., Aadraoui M., Abioui M., Ouchchen M. et al.: *Application of analytical hierarchy process and geophysical method for groundwater potential mapping in the Tata Basin, Morocco*. Water, vol. 14(15), 2022, 2393. https://doi.org/10.3390/w14152393.

[46] Ahmed A., Ranasinghe-Arachchilage Ch., Alrajhi A., Hewa G.: *Comparison of multicriteria decision-making techniques for groundwater recharge potential zonation: Case study of the Willochra Basin, South Australia*. Water (Switzerland), vol. 13(4), 2021, 525. https://doi.org/10.3390/w13040525.

[47] Akkari D.: *L'apport du système d'information géographique(SIG) dans la définition des zones de potentiel hydrique dans le bassin versant Abou Ali (Liban Nord)*. Journal of Alpine Research – Revue de géographie alpine, n. 110-4, 2022, pp. 1–27. https://doi.org/10.4000/rga.10015.
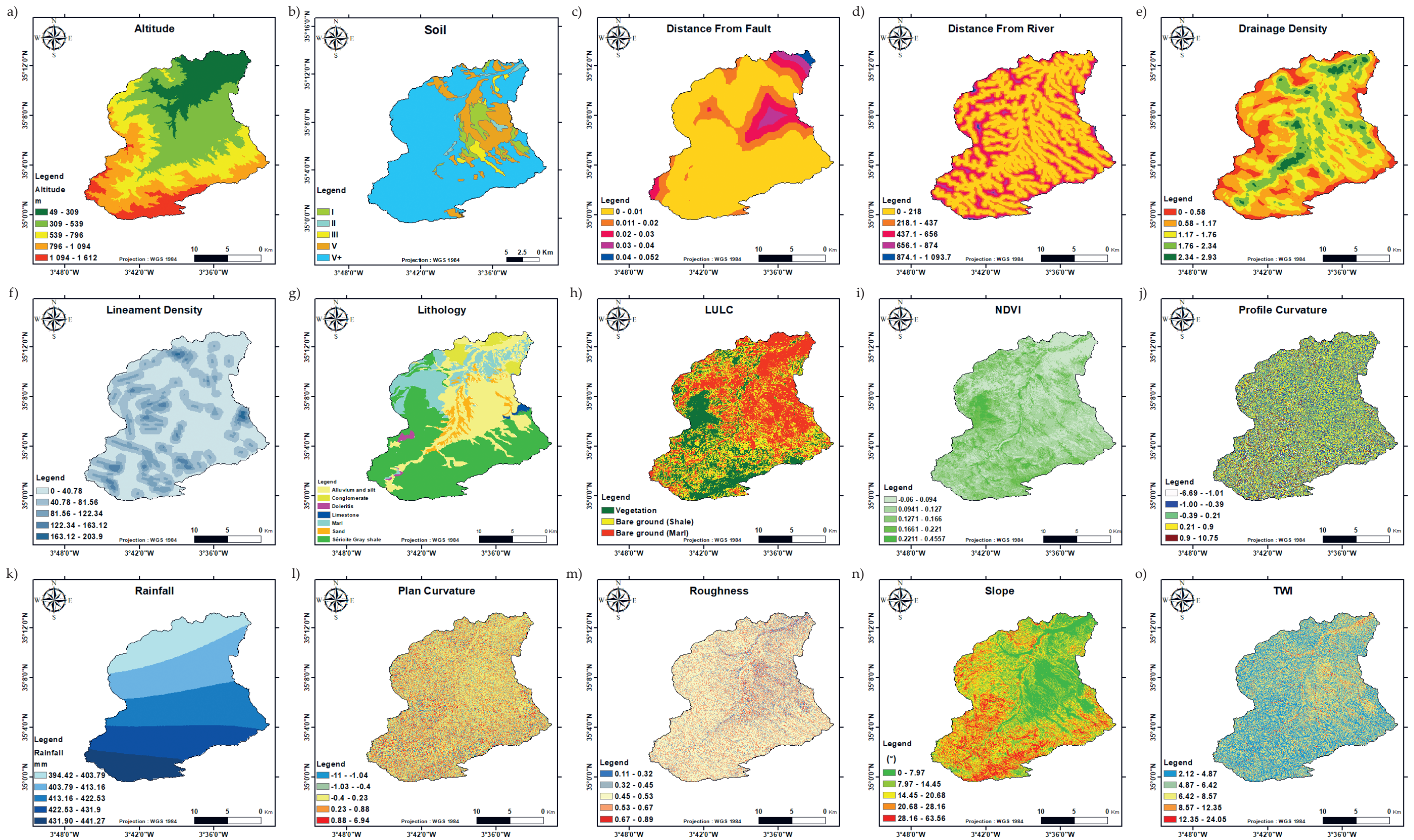
**Fig. 6.** The fifteen-parameters maps used in the current study